

Measurement of Molecular Stopping Cross Sections of Halogen-Carbon Compounds and Calculation of Atomic Stopping Cross Sections of Halogens*

D. Powers, W. K. Chu, R. J. Robinson, and A. S. Lodhi

Baylor University, Waco, Texas 76703

(Received 28 February 1972)

Molecular stopping cross sections ϵ_α of α particles of energy 0.3–2.0 MeV have been measured (probable error 0.9–2.1%) in gaseous (or vapor) CF_4 , C_2F_6 , C_3F_8 , C_4F_8 , CCl_4 , CCl_2F_2 , CHCl_2F , CBrF_3 , $\text{C}_2\text{Br}_2\text{F}_4$, $\text{C}_2\text{H}_3\text{Br}$, $\text{C}_2\text{H}_5\text{Br}$, and $\text{C}_2\text{H}_5\text{I}$. Atomic stopping cross sections for F, Cl, Br, and I have been calculated (probable error 2.3–4.4%) by application of the Bragg additive rule. It is found that carbon $\epsilon(\text{C})$ calculated from gaseous fluorocarbons agrees with previous measurements by Chu and Powers of $\epsilon(\text{C})$ for carbon in solid form but disagrees with $\epsilon(\text{C})$ calculated from gaseous hydrocarbons by Bourland, Chu, and Powers. Consistent results are found by using either of two alternatives: (i) Use hydrocarbon gas $\epsilon(\text{C})$ and experimental $\epsilon_{\text{expt}}(\text{H}_2)$ in hydrogen-enriched C-H-Br or C-H-I compounds, and use solid carbon $\epsilon(\text{C})$ everywhere else; or (ii) use solid carbon $\epsilon(\text{C})$ in all compounds, but use an $\bar{\epsilon}'(\text{H})$ which disagrees by as much as 21% from $\frac{1}{2}\epsilon_{\text{expt}}(\text{H}_2)$. A plot of ϵ_α vs the atomic number Z_2 of the stopping medium shows that the halogen measurements at $Z_2=9, 17, 35,$ and 53 agree well with the existing theory and other experimental measurements for neighboring Z_2 values.

I. INTRODUCTION

Previous experiments^{1–6} have shown the existence of structure when the stopping cross section $\epsilon = dE/Ndx$ of α particles or protons is plotted as a function of the atomic number Z_2 of the stopping medium. Recent calculations⁷ have predicted marked changes in the slope of ϵ vs Z_2 when Z_2 corresponds to a closed-shell atom, i. e., $Z_2=10, 18, 36,$ and 54 . These atomic species are inert and gaseous, and a measurement of ϵ in these substances is quite straightforward. It is desirable to measure ϵ in substances whose Z_2 is contiguous to these noble gases to determine the slope of the curves and to ensure that the ϵ measurements in the noble gases are not fortuitous. Any experiment measuring ϵ in the halogens or alkali metals, however, will be difficult to perform because of the extreme chemical activity of these substances.

A recent experiment⁸ at Baylor University showed that the Bragg rule (viz., the molecular stopping cross section is the additive sum of the stopping cross sections of its atomic constituents) was applicable to hydrocarbon gases whose atoms were single or double bonded, but was not applicable to C_2H_2 whose C atoms were triple bonded. That same experiment gave mild evidence for a physical-state effect, i. e., that ϵ for solid carbon was different from ϵ for carbon calculated by the additive formula for gaseous hydrocarbons.

It was decided then to measure ϵ for the halogens indirectly by first measuring ϵ for several halocarbon compounds and then calculating $\epsilon(\text{F}), \epsilon(\text{Cl}),$ etc., by the additive formula. Thirteen compounds were selected: four fluorocarbons, four chlorocarbons, four bromocarbons, and one iodine compound. The motivation was to have for at least

three of the halocarbons a sufficient number of compounds to ensure internal consistency of the method and of the calculations.

II. EXPERIMENTAL

The experimental method, equipment, and analysis are discussed in two previous papers^{8,9} and are followed here. In brief, an α -particle beam obtained from a 2-MeV Van de Graaff accelerator is passed through a differentially pumped gas-cell system into a 20° analyzing magnet for energy determination. A McLeod gauge (Model GM-100A, Bendix Vacuum Corp., Rochester, N. Y.) measures the pressure of the gaseous halogen compounds admitted into the gas cell. Table I lists the purity, supplier, physical state of all compounds, and vapor pressure of the liquid compounds. Although five of the compounds have impurities as high as 1%, no correction was made for these since Matheson Co. did not specify fractional percentages of these impurities. The same compounds manufactured by other suppliers were not available with purities greater than those of Matheson. When the liquid phase is used, the vapor from this liquid is admitted into the gas cell at a reduced pressure by a fine metering valve. In using the McLeod gauge, care must be taken to ensure that the difference in height of the mercury columns is less than, e. g., 11.5 cm for CCl_4 or 13.8 cm for $\text{C}_2\text{H}_5\text{I}$, so that the gas does not change back to the liquid state and cause sticking of the mercury to the glass capillary of the gauge. The pressure range covered in the experiment was 0.315–2.43 Torr.

No independent dE/dx measurements were made in a separate sealed gas cell in our 18-in. scattering chamber since the two previous experi-

TABLE I. Compounds used in experiment.

Compound	Chemical formula	Minimum purity %	Supplier
Tetrafluoromethane (Freon-14)	CF ₄ (gas) ^a	99.7	Matheson ^b
Hexafluoroethane (Freon-116)	C ₂ F ₆ (gas)	99.6	Matheson
Perfluoropropane	C ₃ F ₈ (gas)	99.0	Matheson
Octafluorocyclobutane (Freon-C-318)	C ₄ F ₈ (gas)	99.99	Matheson
Carbon tetrachloride	CCl ₄ (liquid) ^c	99.99	Baker ^d
Chlorotrifluoromethane (Freon-13)	CClF ₃ (gas)	99.0	Matheson
Dichlorodifluoromethane (Freon-12)	CCl ₂ F ₂ (gas)	99.0	Matheson
Dichlorofluoromethane (Genetron-21)	CHCl ₂ F (gas)	99.0	Matheson
Bromotrifluoromethane (Freon-13B1)	CBrF ₃ (gas)	99.0	Matheson
1,2-Dibromotetrafluoroethane (Freon-114-B2)	C ₂ Br ₂ F ₂ (liquid) ^c	99.5	Matheson
Vinyl bromide	C ₂ H ₃ Br (gas)	99.5	Matheson
Ethyl bromide	C ₂ H ₅ Br (liquid) ^c	99.99	Baker
Ethyl iodide	C ₂ H ₅ I (liquid) ^c	99.99	Baker

^aPhase at atmosphere conditions is listed.

^bMatheson Co., P. O. Box 908, La Porte, Tex. 77571.

^cVapor pressure at room temperature (25 °C) of the liquids was: (i) CCl₄: 115 Torr; (ii) Freon 114-B2: 284 Torr; (iii) C₂H₅Br: 475 Torr; (iv) C₂H₅I: 138 Torr.

^dJ. T. Baker Chemical Co., Phillipsburg, N. J. The reagents listed are "Baker-analyzed reagents" of exceptional high purity.

ments demonstrated that the dE/dx measurements for the two independent systems were identical. All small corrections listed in these prior experiments have been taken into account in the present measurements.

III. RESULTS

A. Analysis

A least-squares curve fit to a fourth-degree polynomial was made to the experimental data points, which varied from $N=141$ to 556 for the various gases, by minimizing the sum

$$\sum_{k=1}^N (\epsilon_k - a_0 - a_1 E_k - a_2 E_k^2 - a_3 E_k^3 - a_4 E_k^4)^2, \quad (1)$$

where ϵ_k is the experimentally measured molecular stopping cross section dE/Ndx at energy E_k . A third-degree polynomial was insufficient to represent the curve, and a fifth-degree polynomial produced no better fit than did the fourth-degree polynomial. The curve fit was carefully checked to ensure that 68% of the points were within plus or minus 1 standard deviation σ of the curve, 96% within plus or minus 2σ of the curve, etc. The curve fit gave a faithful representation of the data

points in all cases except CHCl₂F and C₂H₅I, where the curve was systematically higher than most of the points by 1.5% between 0.3 and 0.5 MeV. This discrepancy was caused by the extremely sensitive nature of the molecular curve fits and was eliminated by curve fitting these two compounds from 0.3 to 1.6 MeV instead of from 0.3 to 2.0 MeV as with the other eleven compounds.

The extremely sensitive nature of the molecular curve fit was also emphasized when atomic-chlorine stopping cross sections were calculated from the molecular-chlorocarbon stopping cross sections by means of the additive formula. Spurious wiggles of small amplitude ($\approx 3\%$) were found around 1.6 MeV in the $\epsilon_{\text{atomic}}^{\text{Cl}}$ -vs- E curve. A small change of 1% in any one of the molecular-chlorocarbon stopping cross sections at 1.6 MeV would change the atomic-chlorine stopping cross section by 2-3%. It was then decided to curve fit the high-energy portion of the data with the function

$$\epsilon_{\alpha} = (C/E) \ln DE, \quad (2)$$

first of all because this form has a physical basis from the Bethe-Bloch formalism, and second, because this form smooths out the spurious wiggles and produces a monotonically decreasing ϵ_{atomic} with energy. Clearly the polynomial curve fit must join smoothly the logarithmic curve fit at some energy E_B . The two curves are discontinuous by as much as 1.9% unless each curve is extended somewhat into the other region. How far the curve is extended into the other region is arbitrary, and our criterion was that the curves must be continuous and the slopes as nearly equal as possible at E_B . This continuity was accomplished by using the polynomial curve fit from 0.3 to 2.0 MeV for all compounds except CHCl₂F and C₂H₅I, where the polynomial curve fit extended from 0.3 to 1.6 MeV. The logarithmic curve fit was made from 1.2 to 2.0 MeV for all compounds except C₂H₃Br, C₂H₅Br, and C₂Br₂F₄, where it was necessary to extend the curve fit from 0.8 to 2.0 MeV in order to obtain a faithful representation of the data points above E_B . The curve-fit parameters so obtained are listed in Table II. A sensitivity test revealed that a polynomial curve fit from $0.3 \leq E \leq E_B$ differed from the polynomial curve fit from $0.3 \leq E \leq 2.0$ MeV by as much as 0.8% for CClF₃, 1.0% for C₂H₅Br, and $\leq 0.6\%$ for the other compounds whose polynomial curve fit extended from 0.3 to 2.0 MeV. A similar sensitivity test showed that a logarithmic curve fit from $E_B \leq E \leq 2.0$ MeV differed by as much as 1.1% for C₂H₃Br at E_B (average difference was 0.44%) and by as much as 0.45% at 2.0 MeV for C₂H₃Br (average difference was 0.17%) from the logarithmic curve which went from 1.2 to 2.0 MeV for ten of the

TABLE II. Curve-fit parameters for $\epsilon = a_0 + a_1E + a_2E^2 + a_3E^3 + a_4E^4$, where ϵ is in 10^{-15} eV cm², E is in MeV, $0.3 \leq E < E_B$, and for $(C/E) \ln(DE)$, where ϵ is in 10^{-15} eV cm², E is in MeV, and $E_B \leq E \leq 2.0$ MeV. E_B is the energy at which the polynomial curve fit is joined smoothly to the logarithmic curve fit. The columns indicating the probable errors in ϵ_{poly} and ϵ_{ln} refer, respectively, to the polynomial curve fit and the logarithmic curve fit.

Gas	a_0	a_1	a_2	a_3	a_4	Probable error in ϵ_{poly} (%)	E_B (MeV)	C	D	Probable error in ϵ_{ln} (%)
CF ₄	110.79	323.65	-321.99	125.15	-18.597	1.63	1.50	174.949	3.68962	1.52
C ₂ F ₆	158.49	598.38	-624.99	250.78	-36.997	1.67	1.26	276.087	3.55414	1.42
C ₃ F ₈	222.41	753.19	-754.55	287.27	-40.21	1.28	1.38	360.518	3.82102	1.61
C ₄ F ₈	272.22	719.12	-689.66	236.58	-27.851	1.01	1.50	397.522	3.72058	0.88
CCl ₄	139.86	1103.90	-1608.00	903.26	-183.17	1.77	1.40	236.284	4.43035	1.73
CClF ₃	122.70	455.65	-519.06	227.84	-36.558	1.47	1.30	199.745	3.54101	1.67
CCl ₂ F ₂	106.64	726.02	-909.13	439.93	-76.861	1.16	1.45	196.968	4.35621	1.42
CHCl ₂ F	112.85	633.89	-839.46	422.58	-76.290	0.93	1.30	162.109	4.82251	1.11
CBrF ₃	128.79	468.43	-500.47	202.65	-29.694	1.31	1.30	212.065	3.61547	1.03
C ₂ Br ₂ F ₄	224.76	723.21	-737.85	274.46	-34.813	1.19	1.30	376.717	3.29325	1.03
C ₂ H ₅ Br	70.193	648.14	-844.35	415.87	-72.370	1.15	1.15	140.609	4.65021	1.09
C ₂ H ₅ I	68.84	781.94	-1049.2	535.82	-96.958	1.59	1.15	152.075	4.80732	1.72
C ₂ H ₅ I	82.66	917.94	-1288.2	708.60	-142.43	1.06	1.30	170.322	5.15676	2.08

compounds and from 0.8 to 2.0 MeV for the remaining three compounds. This sensitivity of the curve fit, depending on how much overlapping is necessary, is essentially uncontrollable. Either the curves join discontinuously by as much as 1.9% (a physically unjustifiable situation), or there is some slight change in the curve caused by the overlapping. The ultimate validity of any curve fit is determined by how faithfully the curve represents the experimental data points. The curve fits of Table II do give a faithful representation of all experimental points, viz., 68% within $\pm\sigma$, 96% within $\pm 2\sigma$ of the curves over the energy interval $0.3 \leq E \leq E_B$ for the polynomial and $E_B \leq E \leq 2.0$ MeV for the logarithmic curve fit.

In Table II is also listed the probable error of each curve which was calculated by $0.6745(\sigma/\epsilon_{\text{expt}}) \times 100\%$, where

$$\sigma = \left[\sum_{k=1}^n (\epsilon_{\text{curve}} - \epsilon_k)^2 / (n - m - 1) \right]^{1/2}$$

$$\bar{\epsilon}_{\text{expt}} = \left(\sum_{k=1}^n \epsilon_k \right) / n$$

and n is the number of experimental points in $0.3 \text{ MeV} \leq E \leq E_B$ for the polynomial curve fit $\epsilon_{\text{curve}}^{\text{poly}}$ or the number of points in $E_B \leq E \leq 2.0$ MeV for the logarithmic curve fit $\epsilon_{\text{curve}}^{\text{ln}}$. m is the degree of freedom for the curve fit: For the fourth-degree polynomial $m = 5$, and for the logarithmic curve $m = 2$.

The curve-fit parameters of Table II have been used to calculate the stopping cross section of the thirteen molecular substances at 100-keV intervals, and the results are presented in Table III.

A typical experimental result is given in Fig. 1 for ϵ_α of CCl₄. The dots are the experimental points, the solid curve the polynomial curve fit, the dashed curve the logarithmic curve fit, and E_B the joining energy. The high-energy point \times at 2 MeV is due to Palmer¹⁰ and was obtained by differentiating her range-energy curve of α particles in CCl₄ vapor. Palmer's measurement is 3.5% lower than our value at 2 MeV. The '+'s below 300 keV are due to Phillips¹¹ for protons in CCl₄ and were converted to α -particle stopping cross sections by using the ratio $\epsilon_\alpha/\epsilon_p$ of Whaling¹² for particles of the same velocity. Phillips's measurement at 280 keV is low by 10.6%, but the calculation using $\epsilon_\alpha/\epsilon_p$ is no better than 10–20%.

B. Fluorine

Table II shows that the probable error of the CF₄, C₂F₆, C₃F₈, and C₄F₈ measurements is from 0.88 to 1.67%. There are six combinations from which either the $\epsilon(C)$ or the $\epsilon(F)$ may be calculated by the additive formula: (a) CF₄-C₂F₆, (b) CF₄-C₃F₈, (c) CF₄-C₄F₈, (d) C₂F₆-C₃F₈, (e) C₂F₆-C₄F₈, and (f) C₃F₈-C₄F₈. The combination yielding the most accurate $\epsilon(F)$ and $\epsilon(C)$ is combination (c), CF₄-C₄F₈. $\epsilon(F)$ has a probable error $\Delta\epsilon(F) \approx 4\%$ and $\epsilon(C)$ a probable error $\Delta\epsilon(C) \approx 12\%$. The least accurate $\epsilon(F)$ and $\epsilon(C)$ are found from combination (d), C₂F₆-C₃F₈. $\epsilon(F)$ has a probable error $\Delta\epsilon(F) \approx 20\%$, and $\Delta\epsilon(C)$ is as bad as 100–300% for this case. A weighted average $\bar{\epsilon}(F)$ or $\bar{\epsilon}(C)$ may be obtained by using $w_i^C = [\Delta\epsilon_i(C)]^{-2}$ and $w_i^F = [\Delta\epsilon_i(F)]^{-2}$, where the index i varies from 1 to 6 and corresponds to the six combinations. $\bar{\epsilon}(F)$ varies in probable error from

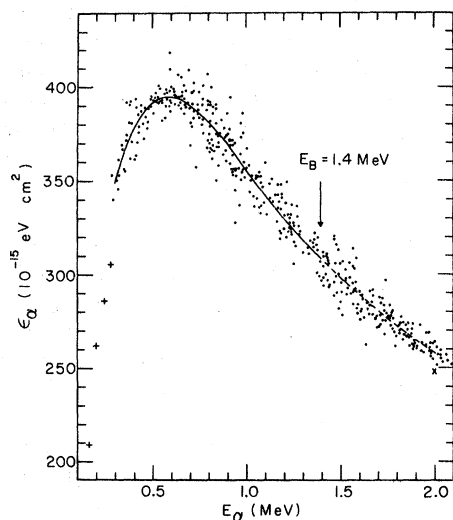


FIG. 1. Molecular stopping cross section ϵ_α as a function of energy E_α for CCl_4 vapor. The dots are the present experimental measurements. The solid curve from 0.3 to $E_B = 1.4$ MeV and the dashed curve from $E_B = 1.4$ to 2.0 MeV represent, respectively, the polynomial curve fit and logarithmic curve fit with parameters given in Table II. The point \times at 2.0 MeV is due to Palmer (Ref. 10) and the $+$'s below 0.3 MeV are Phillips's proton measurements (Ref. 11) converted to α -particle stopping cross sections by using the ratio $\epsilon_\alpha/\epsilon_p$ of Whaling (Ref. 12).

3.9% at 0.3 MeV to 3.4% at 2.0 MeV. $\Delta\bar{\epsilon}(C)$ varies from 10.2% at 0.3 MeV up to 12.4% at 1.4 MeV and then down to 11.7% at 2.0 MeV.

In order for the measurements and the calculations to be internally self-consistent, the six $\epsilon_i(F)$ values should overlap within their indicated error bars, and so should the six $\epsilon_i(C)$ values. This is found to be the case for all $\epsilon_i(F)$ at energies ≥ 0.5 MeV and for three of the $\epsilon_i(C)$. Those combinations for which the error bars do not overlap all involve the compound perfluoropropane C_3F_8 . The supply cylinder of this gas was returned to the manufacturer for chemical analysis of the contents, and a fresh cylinder was simultaneously obtained. The experiment was rerun with the new cylinder, and the same identical curve was obtained as before. The chemical analysis by the manufacturer confirmed the 99% minimum purity, and that the 1% contamination consisted mainly of CO_2 , N_2 , and O_2 , although no numerical percentage of these contaminants was provided. Since these contaminants have lower molecular weight than the C_3F_8 , they would tend to make the $\epsilon(\text{C}_3\text{F}_8)$ measurement lower than it should be. We therefore ran a test calculation by increasing the $\epsilon(\text{C}_3\text{F}_8)$ everywhere by 1%, and all $\epsilon_i(F)$ and $\epsilon_i(C)$ calculations were then consistent at all energies with overlapping error bars. It should be emphasized

TABLE III. Molecular stopping cross sections in 10^{-15} eV cm^2 for the thirteen compounds used in the experiment. The values are obtained from the curve-fit parameters listed in Table II.

Energy (MeV)	CF_4	C_2F_6	C_3F_8	C_4F_8	CCl_4	CCl_2F_2	CClF_3	CCl_2F_2	CHCl_2F	CBrF_3	$\text{C}_2\text{Br}_2\text{F}_4$	$\text{C}_2\text{H}_3\text{Br}$	$\text{C}_2\text{H}_5\text{Br}$	C_2H_4
0.3	182.1	288.2	387.9	432.0	349.2	218.5	253.9	238.3	229.5	382.4	199.3	222.7	260.1	
0.4	196.3	312.9	420.3	464.0	377.3	235.6	277.8	257.2	248.3	412.7	219.1	245.6	285.4	
0.5	206.6	330.5	443.8	487.2	391.3	247.0	292.6	268.0	261.4	434.0	230.6	258.4	299.3	
0.6	213.7	341.9	459.5	502.9	394.7	253.7	300.0	272.4	269.6	447.8	235.6	263.5	304.3	
0.7	218.0	348.2	468.8	512.1	390.5	256.7	301.8	271.9	273.8	455.2	235.4	262.6	302.9	
0.8	220.1	350.4	472.7	515.8	381.3	256.7	299.4	267.8	274.8	457.4	231.6	257.5	297.0	
0.9	220.3	349.3	472.1	515.0	369.2	254.5	293.9	261.4	273.2	455.2	225.3	249.7	288.5	
1.0	219.0	345.7	468.1	510.4	355.8	250.6	286.6	253.6	269.7	449.8	217.5	240.4	278.6	
1.1	216.5	340.1	461.4	502.9	342.5	245.6	278.2	245.1	264.7	441.8	209.0	230.7	268.3	
1.2	213.2	333.2	452.7	493.1	330.0	239.9	269.5	236.7	258.8	432.2	201.4	222.1	258.3	
1.3	209.2	325.0	442.7	481.8	318.7	234.0	261.0	228.7	252.4	421.5	194.6	214.4	248.9	
1.4	204.8	316.4	431.8	469.4	308.0	228.4	253.1	221.1	245.6	411.3	188.2	207.1	240.5	
1.5	200.0	308.0	419.6	456.6	298.3	222.4	246.5	213.8	239.0	401.2	182.1	200.3	232.3	
1.6	194.1	299.9	408.0	443.2	289.2	216.5	239.0	207.0	232.6	391.3	176.4	193.9	224.6	
1.7	189.0	292.1	396.8	431.3	280.6	210.9	232.0	200.6	226.5	381.7	171.0	187.9	217.5	
1.8	184.0	284.7	386.2	420.0	272.5	205.5	225.4	194.6	220.7	372.5	166.0	182.3	210.8	
1.9	179.3	277.5	376.1	409.2	264.9	200.4	219.1	189.0	215.1	363.6	161.2	177.0	204.6	
2.0	174.8	270.7	366.6	398.9	257.7	195.5	213.2	183.7	209.8	355.1	156.8	172.1	198.7	

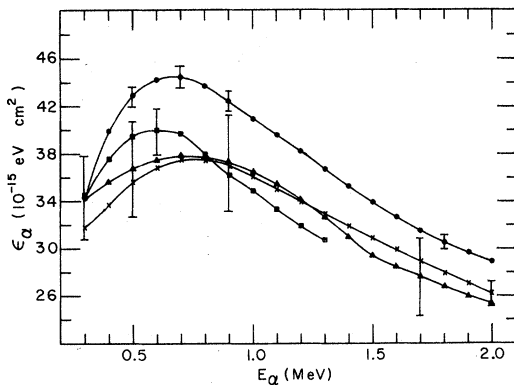


FIG. 2. Atomic stopping cross sections ϵ_{α} as a function of energy E_{α} for carbon. The \times 's are solid-carbon measurements of Chu and Powers (Ref. 5). The \blacksquare 's are solid-carbon measurements of Porat and Ramavataram (Ref. 13). The \bullet 's are calculated by application of Bragg's rule to gaseous-hydrocarbon molecular stopping cross sections (Ref. 8). The \blacktriangle 's are weighted averages of $\bar{\epsilon}(C)$ calculated from gaseous fluorocarbons by the technique in Sec. III B.

that the original weighted averages $\bar{\epsilon}(F)$ and $\bar{\epsilon}(C)$ differ by only 0.07 and 0.14%, respectively, from weighted averages obtained by increasing $\epsilon(C_3F_8)$ by 1%. The reason for this extremely small change is that the weighting process, by its very nature, emphasizes the combination CF_4 - C_4F_8 much more than any of the other combinations. We therefore conclude that a contamination of the C_3F_8 by no more than 1% is likely, but that it will affect our weighted averages by no more than 0.07–0.14%. We have tabulated the *uncorrected* $\epsilon(C_3F_8)$ measurements in Tables II and III, since the manufacturer did not provide fractional percentages for the indicated contaminants.

In Fig. 2 we have plotted the weighted average $\bar{\epsilon}(C)$ (probable error 10.2–12.4%) obtained from the fluorocarbons as solid triangles and have compared this to the solid-carbon measurements⁵ of Chu and Powers (plotted as \times 's and having probable errors 4.2%), to Porat and Ramavataram's solid-carbon measurements¹³ (plotted as \blacksquare 's and with probable error 5%), and to the "gas carbon" of Bourland *et al.*⁸ (plotted as \bullet 's and with probable error 1.6–2.0%) calculated from α -particle stopping cross sections in gaseous hydrocarbons. *The completely surprising result is that the weighted average $\bar{\epsilon}(C)$ from the gaseous fluorocarbons agrees with the solid-carbon measurements $\epsilon(C)$ (both Chu and Powers and also Porat and Ramavataram) everywhere within experimental accuracy, but disagrees with "gas carbon" $\epsilon(C)$ calculated from gaseous hydrocarbons over the energy region 0.5–0.9 MeV. One would have a priori thought that if "gas-carbon" $\epsilon(C)$ calculated from gaseous hydrocarbons differed by up to 22%*

from solid-carbon $\epsilon(C)$, then "gas-carbon" $\epsilon(C)$ calculated from gaseous fluorocarbons would have disagreed with solid $\epsilon(C)$ in a similar manner.

As a check to ensure that the original gaseous-hydrocarbon measurements were not fortuitous, we measured ϵ_{α} of α particles in the hydrocarbon 1-butene, C_4H_8 , which was heavier than any hydrocarbon measured by Bourland *et al.* The additive sum of $\epsilon(H_2)$ and "gas-carbon" $\epsilon(C)$ calculated from the previous gaseous-hydrocarbon stopping cross sections agreed completely with the new ϵ measurements in 1-butene, C_4H_8 , thereby substantiating the original hydrocarbon measurements. This result seems to imply that a different $\epsilon(C)$ must be used in gaseous fluorocarbons than in gaseous hydrocarbons which otherwise have the same molecular structure, e.g., CH_4 and CF_4 , or C_2H_6 and C_2F_6 . [It might be argued that since 1-butene, C_4H_8 , has a different molecular structure than octafluorocyclobutane, C_4F_8 , the difference in molecular structure could account for the difference. In the hydrocarbon-gas experiment, however, the two isomers propylene, C_3H_6 , and cyclopropane, $(CH_2)_3$, had identical stopping cross sections from 0.3 to 2.0 MeV, so there is little reason to expect the molecular structure to account for the difference here.]

One might also argue that the *same* $\epsilon(C)$ should be used in both gaseous fluorocarbons and gaseous hydrocarbons, and that the problem lies not with $\epsilon(C)$ but with $\epsilon(H)$. This possibility, of course, exists. The reason that Bourland and Powers⁸ assumed the problem was with $\epsilon(C)$ was because when they applied Bragg's rule to $\epsilon(CH_4)$, $\epsilon(C_2H_4)$, $\epsilon(C_2H_6)$, $\epsilon(C_3H_8)$, and $\epsilon((CH_2)_3)$ and solved any pair of equations simultaneously, they obtained an $\epsilon(H)$ which was precisely one-half the experimentally measured molecular stopping cross section $\epsilon(H_2)$. This finding seemed to point to something being wrong with $\epsilon(C)$, since the value calculated from the pairs of simultaneous equations disagreed by up to 22% from the measured solid $\epsilon(C)$. Also the physical state of hydrogen and gas hydrocarbons was the same, whereas the physical state was different for the carbon and the hydrocarbons. The measurement of $\epsilon(H_2)$ was made in two entirely separate systems (a transmission experiment using a differentially pumped gas cell and a reflection experiment where the reflected α particles went through a small gas cell with Ni end windows and on into a surface barrier detector) with identical results. These separate measurements should enhance the reliability of the $\epsilon(H_2)$ result. If it is assumed that $\epsilon(C)$ is solid $\epsilon(C)$ everywhere, then we can obtain an $\epsilon(H)$ from the hydrocarbon gases as follows:

$$\epsilon'_1(H) = \frac{1}{4}[\epsilon(CH_4) - \epsilon(C)] ,$$

$$\epsilon'_2(H) = \frac{1}{4}[\epsilon(C_2H_4) - 2\epsilon(C)] ,$$

$$\epsilon'_3(\text{H}) = \frac{1}{6} [\epsilon(\text{C}_2\text{H}_6) - 2\epsilon(\text{C})],$$

$$\epsilon'_4(\text{H}) = \frac{1}{6} [\epsilon(\text{C}_3\text{H}_8) - 3\epsilon(\text{C})],$$

and

$$\epsilon'_5(\text{H}) = \frac{1}{6} [\epsilon((\text{CH}_2)_3) - 3\epsilon(\text{C})].$$

The weighted average $\bar{\epsilon}'(\text{H})$ of these five values [using Chu and Powers's solid $\epsilon(\text{C})$ which has a probable error of $\pm 4.2\%$] has a probable error of $\pm 3.5\%$ at 0.4 MeV to $\pm 5.2\%$ at 2.0 MeV, and disagrees with $\frac{1}{2}\epsilon_{\text{expt}}(\text{H}_2)$ by from 20.8% at 0.4 MeV to 13.3% at 1.7 MeV. In Fig. 3 we plot $\bar{\epsilon}'(\text{H})$ vs E_α as the dashed curve, and the experimental $\frac{1}{2}\epsilon_{\text{expt}}(\text{H}_2)$ vs E_α is plotted as the solid curve. From the above, we see that a Bragg-rule calculation of gaseous hydrocarbons either gives an $\epsilon(\text{C})$ which disagrees from measured solid $\epsilon(\text{C})$ by as much as 22%, or else gives an $\epsilon(\text{H})$ which disagrees by about the same amount from the measured $\frac{1}{2}\epsilon_{\text{expt}}(\text{H}_2)$. It was thought that $\epsilon(\text{C})$ was off because of the agreement between the calculated $\epsilon(\text{H})$ and the measured $\frac{1}{2}\epsilon_{\text{expt}}(\text{H}_2)$, but the present findings with gas fluorocarbons seem to weaken that conclusion somewhat. One thing seems fairly clear, however, and that is, if $\epsilon(\text{C})$ is different for gas fluorocarbons and gas hydrocarbons, the difference is certainly not a physical-state effect as was mildly implied by Bourland and Powers.⁸

In what follows in the remaining sections of this paper the analysis is made under the assumption that gaseous hydrocarbon $\epsilon(\text{C})$ is different from solid carbon $\epsilon(\text{C})$, and that $\epsilon(\text{H}) = \frac{1}{2}\epsilon_{\text{expt}}(\text{H}_2) = \frac{1}{2}\epsilon(\text{H}_2)$. At the same time, however, the alternate possibility is considered that $\epsilon(\text{C})$ is the same as solid carbon $\epsilon(\text{C})$ everywhere, and that $\epsilon(\text{H}) = \bar{\epsilon}'(\text{H})$.

The above discovery that $\epsilon(\text{C})$ in gaseous fluorocarbons is the same as solid $\epsilon(\text{C})$ then enables one to make a different analysis of the fluorocarbon data, viz., use the solid $\epsilon(\text{C})$ previously obtained by Chu and Powers or by Porat and Ramavartaram to calculate $\epsilon(\text{F})$ from $\epsilon(\text{CF}_4)$, $\epsilon(\text{C}_2\text{F}_6)$, $\epsilon(\text{C}_3\text{F}_8)$, and $\epsilon(\text{C}_4\text{F}_{10})$ by the additive formula. This procedure was used, and each of the four $\epsilon_i(\text{F})$'s so obtained agreed within experimental accuracy with each other and also with the weighted average $\bar{\epsilon}(\text{F})$ previously obtained. Had the above result been known in the initial stages of the experiment, it would have been necessary to measure only one molecular fluorocarbon, say $\epsilon(\text{CF}_4)$, and then calculate $\epsilon(\text{F})$ by subtracting solid $\epsilon(\text{C})$ and dividing the result by four. As expected, an $\epsilon(\text{F})$ calculated from the "gas-carbon" $\epsilon(\text{C})$ and the four fluorocarbon ϵ 's disagrees by as much as 6.4% from the weighted average $\bar{\epsilon}(\text{F})$, which is outside the experimental error.

The weighted average $\bar{\epsilon}(\text{F})$, with probable error 3.4–3.9%, is tabulated in Table IV.

C. Chlorine

In principle, one need only measure $\epsilon(\text{CCl}_4)$ and then obtain $\epsilon(\text{Cl})$ by $\frac{1}{4}[\epsilon(\text{CCl}_4) - \epsilon(\text{C})]$ if $\epsilon(\text{C})$ is known. If the $\bar{\epsilon}(\text{C})$ of probable error 10.2–12.4% of Sec. III B is used, an $\epsilon(\text{Cl})$ of probable error $\approx 2.3\%$ still can be calculated from the additive formula. The reason for the relatively high accuracy is the high chlorine content in CCl_4 which makes the dependence upon carbon small.

In light of the findings of Sec. III B, however, some ambiguity exists as to whether $\epsilon(\text{C})$ of solid media or $\epsilon(\text{C})$ from gaseous hydrocarbons should be used, since the latter is up to 22% higher than the former. Also, there exists the slight possibility that $\epsilon(\text{C})$ from gaseous chlorocarbons may even be different from either of the other two. As it turns out, $\epsilon(\text{Cl})$ changes by no more than 1.4% depending on whether solid $\epsilon(\text{C})$ or gaseous hydrocarbon $\epsilon(\text{C})$ is used in the calculation. A 1% systematic error in $\epsilon(\text{CCl}_4)$, however, will be reflected as a 1.4% change in $\epsilon(\text{Cl})$, and several small changes [wrong $\epsilon(\text{C})$ being used, small systematic errors in the $\epsilon(\text{CCl}_4)$ measurement] could, in principle, change $\epsilon(\text{Cl})$ by several percent. The measurement of several chlorocarbon compounds should help eliminate some of these pathological possibilities.

Molecular stopping cross sections were obtained for gaseous CCl_4 (CCl_4 in vapor phase), CCl_3F , CCl_2F_2 , and CHCl_2F . Three independent $\epsilon_i(\text{C})$, errors, $\Delta\epsilon_i(\text{C})$ from 29 to 87%, were calculated and a weighted average $\bar{\epsilon}(\text{C})$ of probable error 27–58% was calculated in the same manner as Sec. III B.

TABLE IV. Atomic stopping cross sections for the halogens as calculated from the halocarbon compounds; ϵ is in 10^{-15} eV cm^2 : The percentage probable error is given in parentheses.

Energy (MeV)	$\bar{\epsilon}(\text{F})$	$\bar{\epsilon}(\text{Cl})$	$\bar{\epsilon}(\text{Br})$	$\epsilon(\text{I})$
0.3	36.9(3.9%)	76.8(3.5%)	88.7(2.8%)	125.2(2.6%)
0.4	40.1(3.9%)	83.8(2.3%)	95.5(2.9%)	135.6(2.6%)
0.5	42.5(3.9%)	87.4(2.3%)	99.7(3.0%)	141.2(2.7%)
0.6	44.1(3.9%)	88.4(2.3%)	102.2(3.0%)	143.9(2.7%)
0.7	45.1(3.9%)	87.6(2.4%)	102.9(3.0%)	143.9(2.6%)
0.8	45.6(3.8%)	85.6(2.4%)	102.5(3.0%)	142.3(2.6%)
0.9	45.8(3.8%)	82.8(2.5%)	100.4(3.0%)	138.9(2.6%)
1.0	45.6(3.8%)	79.6(2.5%)	97.7(3.0%)	134.8(2.6%)
1.1	45.2(3.8%)	76.5(2.6%)	94.1(3.0%)	130.1(2.6%)
1.2	44.7(3.8%)	73.6(2.6%)	91.2(2.9%)	125.9(2.6%)
1.3	44.0(3.7%)	71.1(2.6%)	88.8(2.8%)	122.6(4.4%)
1.4	43.3(3.7%)	68.7(2.6%)	86.8(2.8%)	119.6(4.4%)
1.5	42.4(3.4%)	66.8(2.4%)	84.7(2.7%)	116.5(4.4%)
1.6	41.3(3.4%)	64.7(2.5%)	82.7(2.7%)	113.5(4.3%)
1.7	40.2(3.4%)	62.7(2.8%)	81.2(2.6%)	111.0(4.3%)
1.8	39.2(3.4%)	60.8(3.1%)	79.2(2.6%)	108.1(4.2%)
1.9	38.2(3.4%)	59.1(3.4%)	77.4(2.6%)	105.2(4.2%)
2.0	37.3(3.4%)	57.5(3.5%)	75.5(2.5%)	102.4(4.2%)

All $\epsilon_i(\text{C})$ error bars overlapped everywhere except at 0.3 MeV. The weighted-average error bars overlap solid $\epsilon(\text{C})$ and gaseous-hydrocarbon $\epsilon(\text{C})$ everywhere, but the $\bar{\epsilon}(\text{C})$ trend follows more closely that of solid $\epsilon(\text{C})$ than that of gaseous-hydrocarbon $\epsilon(\text{C})$. Certainly there is no evidence to substantiate that $\epsilon(\text{C})$ from chlorocarbons is different from that calculated from fluorocarbons.

Only two $\epsilon_i(\text{F})$'s can be calculated from the four gaseous compounds CCl_4 , CClF_3 , CCl_2F_2 , and CHCl_2F . Both $\epsilon_i(\text{F})$ and their weighted average agree everywhere except at 0.3 MeV with the $\bar{\epsilon}(\text{F})$ from the four fluorocarbons of Sec. III B.

Three $\epsilon_i(\text{Cl})$'s can be calculated (method 1) from the four compounds:

$$(a) \epsilon_1(\text{Cl}) = \frac{1}{2}\epsilon(\text{CCl}_4) - \epsilon(\text{CHCl}_2\text{F}) + \frac{1}{2}\epsilon(\text{CCl}_2\text{F}_2) + \frac{1}{2}\epsilon(\text{H}_2),$$

$$(b) \epsilon_2(\text{Cl}) = \frac{2}{3}\epsilon(\text{CCl}_4) - \epsilon(\text{CHCl}_2\text{F}) + \frac{1}{3}\epsilon(\text{CClF}_3) + \frac{1}{2}\epsilon(\text{H}_2),$$

and

$$(c) \epsilon_3(\text{Cl}) = 2\epsilon(\text{CCl}_2\text{F}_2) - \epsilon(\text{CClF}_3) - \epsilon(\text{CHCl}_2\text{F}) + \frac{1}{2}\epsilon(\text{H}_2).$$

An $\epsilon(\text{Cl})$ cannot be obtained from the combination CCl_4 , CCl_2F_2 , and CClF_3 because the simultaneous equations of this combination are dependent. $\Delta\epsilon_1(\text{Cl})$ varies from 5.3 to 5.7%, $\Delta\epsilon_2(\text{Cl})$ from 5.9 to 6.1%, and $\Delta\epsilon_3(\text{Cl})$ from 11 to 13%. The weighted average $\bar{\epsilon}(\text{Cl})$ has an uncertainty of 5.3–5.7%. All $\epsilon_i(\text{Cl})$'s and $\bar{\epsilon}(\text{Cl})$ agree everywhere within their error bars except at 0.3 MeV.

It is suspected that the disagreement of the $\epsilon_i(\text{C})$'s, $\epsilon_i(\text{F})$'s, and $\epsilon_i(\text{Cl})$'s at 0.3 MeV is due to the sensitivity of the curve fits. From Table I all chlorocarbons except CCl_4 have a purity no better than 99.0%. An increase in $\epsilon(\text{CCl}_2\text{F}_2)$ by 0.7%, for example, brings all calculated ϵ 's [$\epsilon_i(\text{C})$, $\epsilon_i(\text{F})$, $\epsilon_i(\text{Cl})$] into agreement at 0.3 MeV without destroying the agreement elsewhere.

Because there always exists the possibility of some small unknown systematic error in $\epsilon(\text{CCl}_4)$, we decided to obtain our value of $\epsilon(\text{Cl})$ by subtraction by what we call method 2: We used the $\bar{\epsilon}(\text{C})$ and $\bar{\epsilon}(\text{F})$ calculated from the four gaseous fluorocarbon compounds along with $\frac{1}{2}\epsilon(\text{H}_2)$ measured in Ref. 8 to calculate $\epsilon_i(\text{Cl})$ by direct subtraction from the four chlorocarbons, i. e.,

$$(a) \epsilon_1(\text{Cl}) = \frac{1}{4}[\epsilon(\text{CCl}_4) - \bar{\epsilon}(\text{C})],$$

$$(b) \epsilon_2(\text{Cl}) = \frac{1}{2}[\epsilon(\text{CHCl}_2\text{F}) - \frac{1}{2}\epsilon(\text{H}_2) - \bar{\epsilon}(\text{F}) - \bar{\epsilon}(\text{C})],$$

$$(c) \epsilon_3(\text{Cl}) = \epsilon(\text{CClF}_3) - 3\bar{\epsilon}(\text{F}) - \bar{\epsilon}(\text{C}),$$

and

$$(d) \epsilon_4(\text{Cl}) = \frac{1}{2}[\epsilon(\text{CCl}_2\text{F}_2) - \bar{\epsilon}(\text{C}) - 2\bar{\epsilon}(\text{F})].$$

All error bars overlap except at 0.3 MeV. A weighted average $\bar{\epsilon}(\text{Cl})$ was calculated for these four values and is entered in Table IV as our value of $\bar{\epsilon}(\text{Cl})$. The weighted average $\bar{\epsilon}(\text{Cl})$ by method

2 has a probable error of 2.3–2.6%, and agrees with the weighted average $\bar{\epsilon}(\text{Cl})$ by method 1 to better than 1.2% from 0.3 to 1.4 MeV and from 1.3% at 1.5 MeV to 3.5% at 2.0 MeV. We quote as probable errors for $\bar{\epsilon}(\text{Cl})$ in Table IV those values 2.3–2.6% except at 0.3 MeV (3.5%) and 1.7–2.0 MeV (2.8–3.5%) where the two separate weighted averages agree. The probable error 2.3–3.5% assigned to $\bar{\epsilon}(\text{Cl})$ in Table IV is between the probable error of $\frac{1}{4}[\epsilon(\text{CCl}_4) - \bar{\epsilon}(\text{C})]$ (2.3%) and the weighted average $\bar{\epsilon}(\text{Cl})$ (5.3–5.7%) calculated by method 1. In the above we are essentially using "solid" $\epsilon(\text{C})$ in the calculations. If we use $\bar{\epsilon}'(\text{H})$ instead of $\frac{1}{2}\epsilon_{\text{expt}}(\text{H}_2)$ in the above calculations according to the discussion of Sec. III B, we find that the $\bar{\epsilon}(\text{Cl})$ of method 2 is decreased by $\leq 0.4\%$, which is well within the quoted error bars of Table IV.

D. Bromine

The initial method of approach was to measure $\epsilon(\text{CBrF}_3)$, $\epsilon(\text{C}_2\text{Br}_2\text{F}_4)$, $\epsilon(\text{C}_2\text{H}_3\text{Br})$, and $\epsilon(\text{C}_2\text{H}_5\text{Br})$ and to use the additive formula to solve the four equations simultaneously to obtain $\epsilon(\text{Br})$. For this approach one must use $\epsilon(\text{H}_2)$ or $\bar{\epsilon}'(\text{H})$ in the calculations. Unfortunately, this method yields only two independent values of $\epsilon(\text{Br})$:

$$(a) \epsilon_1(\text{Br}) = 3\epsilon(\text{C}_2\text{Br}_2\text{F}_4) - 4\epsilon(\text{CBrF}_3) - \epsilon(\text{C}_2\text{H}_3\text{Br}) + \frac{3}{2}\epsilon(\text{H}_2)$$

and

$$(b) \epsilon_2(\text{Br}) = 3\epsilon(\text{C}_2\text{Br}_2\text{F}_4) - 4\epsilon(\text{CBrF}_3) - \epsilon(\text{C}_2\text{H}_5\text{Br}) + \frac{5}{2}\epsilon(\text{H}_2).$$

In addition, the error bars on $\epsilon_i(\text{Br})$ vary from 15 to 30%, and the $\epsilon_i(\text{Br})$ -vs-energy curve has a very peculiar shape in that it increases from $\approx 70 \times 10^{-15}$ eV cm² at 0.3 MeV up to $\approx 95 \times 10^{-15}$ eV cm² at 1.1 MeV and remains essentially constant from 1.1 to 2.0 MeV. Because of the large error bars and peculiar shape of $\epsilon_i(\text{Br})$ obtained, we are unable to assign a meaningful $\epsilon(\text{Br})$ by this method (simultaneous-solution method).

Because of the ambiguity in $\epsilon(\text{C})$ discussed in Sec. III B, it is also not clear that a meaningful $\epsilon(\text{Br})$ can be obtained by subtraction of atomic stopping cross sections from the molecular stopping cross sections. Nevertheless, four possibilities exist:

$$(a) \epsilon_1(\text{Br}) = \epsilon(\text{C}_2\text{H}_3\text{Br}) - 2\epsilon(\text{C}) - \frac{3}{2}\epsilon(\text{H}_2),$$

$$(b) \epsilon_2(\text{Br}) = \epsilon(\text{C}_2\text{H}_5\text{Br}) - 2\epsilon(\text{C}) - \frac{5}{2}\epsilon(\text{H}_2),$$

$$(c) \epsilon_3(\text{Br}) = \epsilon(\text{CBrF}_3) - \epsilon(\text{C}) - 3\epsilon(\text{F}),$$

and

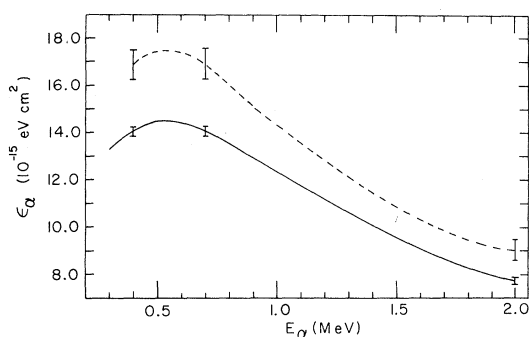


FIG. 3. Atomic stopping cross sections $\epsilon_\alpha(\text{H})$ as a function of energy E_α . Solid curve is one-half the experimental $\epsilon_{\text{exp}}(\text{H}_2)$ measured by Bourland *et al.* (Ref. 8). The dashed curve $\epsilon'(\text{H})$ is calculated by subtracting the solid-carbon $\epsilon(\text{C})$ of Chu and Powers (Ref. 5) from the hydrocarbon stopping cross sections according to the procedure of Sec. III B.

$$(d) \quad \epsilon_4(\text{Br}) = \frac{1}{2}\epsilon(\text{C}_2\text{Br}_2\text{F}_4) - \epsilon(\text{C}) - 2\epsilon(\text{F}) .$$

We used $\bar{\epsilon}(\text{F})$ from Table IV, solid $\epsilon(\text{C})$ measured in Ref. 5, and $\epsilon(\text{H}_2)$ measured in Ref. 8, and the rather surprising results are shown in Fig. 4. The shapes of all four curves are now similar to those in Figs. 1 and 2 (typical ϵ -vs- E shape). However, the two $\epsilon(\text{Br})$ curves calculated from the C-H-Br compounds are higher by as much as 18% than the two $\epsilon(\text{Br})$ curves calculated from C-F-Br compounds. Similar results are obtained if $\epsilon(\text{C})$ gas from Ref. 8 is used in place of solid $\epsilon(\text{C})$, except that the difference in the trends is now approximately 11% at 0.7 MeV. Although in Fig. 4 the error bars overlap everywhere above 1.1 MeV, they do not below 1.1 MeV. The tightness of the two C-H-Br curves and also (below 1.1 MeV) that of the C-F-Br curves is also of interest.

An entirely separate approach can be made in obtaining $\epsilon(\text{Br})$ by using $\epsilon(\text{CBrF}_3)$ and $\epsilon(\text{C}_2\text{Br}_2\text{F}_4)$ along with the four fluorocarbon measurements $\epsilon(\text{CF}_4)$, $\epsilon(\text{C}_2\text{F}_6)$, $\epsilon(\text{C}_3\text{F}_8)$, and $\epsilon(\text{C}_4\text{F}_{10})$ of Sec. III B. If we limit ourselves to no more than two fluorocarbons per calculation, there nevertheless are eight possible $\epsilon_i(\text{Br})$'s obtained, e.g.,

$$\begin{aligned} (a) \quad \epsilon_1(\text{Br}) &= \epsilon(\text{CBrF}_3) - \frac{1}{2}\epsilon(\text{C}_2\text{F}_6) , \\ (b) \quad \epsilon_2(\text{Br}) &= \epsilon(\text{CBrF}_3) - \frac{1}{4}\epsilon(\text{CF}_4) - \frac{1}{4}\epsilon(\text{C}_3\text{F}_8) , \\ (c) \quad \epsilon_3(\text{Br}) &= \epsilon(\text{CBrF}_3) - \frac{1}{2}\epsilon(\text{CF}_4) - \frac{1}{8}\epsilon(\text{C}_4\text{F}_{10}) , \\ (d) \quad \epsilon_4(\text{Br}) &= \epsilon(\text{CBrF}_3) - \frac{1}{2}\epsilon(\text{C}_3\text{F}_8) + \frac{1}{8}\epsilon(\text{C}_4\text{F}_{10}) , \\ (e) \quad \epsilon_5(\text{Br}) &= \frac{1}{2}\epsilon(\text{C}_2\text{Br}_2\text{F}_4) - \frac{1}{4}\epsilon(\text{C}_4\text{F}_{10}) , \end{aligned}$$

etc. Thirteen additional $\epsilon_i(\text{Br})$'s can be obtained by suitable combinations of $\epsilon(\text{C}_2\text{H}_3\text{Br})$, $\epsilon(\text{C}_2\text{H}_5\text{Br})$, $\epsilon(\text{H}_2)$, $\epsilon(\text{CH}_4)$, $\epsilon(\text{C}_2\text{H}_4)$, $\epsilon(\text{C}_2\text{H}_6)$, and $\epsilon(\text{C}_3\text{H}_8)$, where we use the hydrocarbon ϵ 's of Ref. 8. We calculated and plotted the 21 values of $\epsilon_i(\text{Br})$ so

obtained. It was quite clear from this plot that a common trend existed for $\epsilon(\text{Br})$. We divided the 21 curves into four categories, each category related to a molecular-bromine compound. The number of $\epsilon(\text{Br})$ curves per compound were as follows: $\epsilon(\text{CBrF}_3)$, 4 (the first four enumerated above); $\epsilon(\text{C}_2\text{Br}_2\text{F}_4)$, 4; $\epsilon(\text{C}_2\text{H}_3\text{Br})$, 6; and $\epsilon(\text{C}_2\text{H}_5\text{Br})$, 7. The most accurate $\epsilon_i(\text{Br})$ from the 4 categories were

$$(a) \quad \epsilon_1(\text{Br}) = \epsilon(\text{CBrF}_3) - \frac{1}{4}\epsilon(\text{CF}_4) - \frac{1}{4}\epsilon(\text{C}_3\text{F}_8) \quad [\pm (2.7-4\%)] ,$$

$$(b) \quad \epsilon_2(\text{Br}) = \frac{1}{2}\epsilon(\text{C}_2\text{Br}_2\text{F}_4) - \frac{1}{4}\epsilon(\text{C}_4\text{F}_{10}) \quad [\pm (2-3\%)] ,$$

$$(c) \quad \epsilon_3(\text{Br}) = \epsilon(\text{C}_2\text{H}_3\text{Br}) - \epsilon(\text{C}_2\text{H}_4) + \frac{1}{2}\epsilon(\text{H}_2) \quad [\pm (2.1-3.3\%)] ,$$

and

$$(d) \quad \epsilon_4(\text{Br}) = \epsilon(\text{C}_2\text{H}_5\text{Br}) - \frac{1}{2}\epsilon(\text{CH}_4) - \frac{1}{2}\epsilon(\text{C}_3\text{H}_8) \quad [\pm (3.2-4.4\%)] .$$

The error bars in these curves overlapped everywhere, and their weighted average had an uncertainty of $\pm (1.6-1.8\%)$. We next took the least accurate $\epsilon(\text{Br})$'s from the four categories and checked the consistency. The error bars for these least accurate curves [$\pm (3.7-9\%)$] also overlapped everywhere, and their weighted average had an uncertainty of $\pm (3.1-3.7\%)$.

In the above approach we are essentially using the "solid-carbon" $\epsilon(\text{C})$ [or fluorocarbon $\epsilon(\text{C})$] in the C-Br-F stopping-cross-section measurements

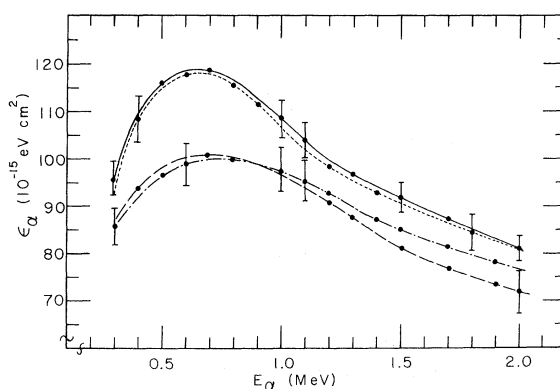


FIG. 4. Atomic stopping cross sections $\epsilon_\alpha(\text{Br})$ as a function of energy E_α . Solid $\epsilon(\text{C})$ from Ref. 5, $\epsilon(\text{H}_2)$ from Ref. 8, and $\bar{\epsilon}(\text{F})$ from Table IV are used to calculate: solid curve, $\epsilon(\text{C}_2\text{H}_3\text{Br}) - 2\epsilon(\text{C}) - \frac{5}{8}\epsilon(\text{H}_2)$; dotted curve, $\epsilon(\text{C}_2\text{H}_5\text{Br}) - 2\epsilon(\text{C}) - \frac{5}{8}\epsilon(\text{H}_2)$; dashed curve, $\epsilon(\text{CBrF}_3) - \epsilon(\text{C}) - 3\bar{\epsilon}(\text{F})$; and dot-dashed curve, $\frac{1}{2}\epsilon(\text{C}_2\text{Br}_2\text{F}_4) - \epsilon(\text{C}) - 2\bar{\epsilon}(\text{F})$. It is seen that $\epsilon(\text{Br})$ calculated from the hydrogen-enriched $\text{C}_2\text{H}_3\text{Br}$ and $\text{C}_2\text{H}_5\text{Br}$ is systematically higher than $\epsilon(\text{Br})$ calculated from C-F-Br compounds.

and the gaseous-hydrocarbon $\epsilon(C)$ in the C-H-Br stopping-cross-section measurements. The two higher curves of Fig. 4 are brought into very close agreement with the two lower curves (all error bars overlap everywhere) if the hydrocarbon-gas-carbon $\epsilon(C)$ is used instead of the solid-carbon $\epsilon(C)$ in the C-H-Br compounds. We used these corrected upper curves of Fig. 4 with the two uncorrected lower curves to obtain a weighted average $\bar{\epsilon}(\text{Br})$. The weighted average is uncertain from $\pm(2.5-3.0\%)$ and is tabulated as $\bar{\epsilon}(\text{Br})$ in Table IV. This latter weighted average agrees everywhere with the weighted average of all 21 combinations, with the weighted average of the four combinations giving the least error, and with the weighted average of the four combinations giving the most error.

From the discussion of Sec. IIIB the alternative exists that solid $\epsilon(C)$ should be used everywhere and that $\bar{\epsilon}'(\text{H})$ should be used in place of $\frac{1}{2}\epsilon_{\text{expt}}(\text{H}_2)$. The four values of $\epsilon_i(\text{Br})$ were calculated by the subtraction method mentioned at the beginning of Sec. IIID, and an $\bar{\epsilon}(\text{Br})$ was obtained. It was found that the new $\bar{\epsilon}(\text{Br})$ agreed everywhere within 0.6% to the $\bar{\epsilon}(\text{Br})$ values tabulated in Table IV. $\epsilon_1(\text{Br})$ differs, however, by as much as 10% from $\epsilon_4(\text{Br})$ in this new approach, and the error bars failed to overlap by as much as 1.1% below 0.8 MeV. An increase in $\epsilon(\text{C}_2\text{Br}_2\text{F}_4)$ by 0.5% (which may be needed since $\text{C}_2\text{Br}_2\text{F}_4$ is only 99.5% pure according to Table I) will cause all error bars for all four curves to overlap everywhere.

One is therefore faced with the following dilemma: (i) The use of hydrocarbon gas $\epsilon(C)$ and $\epsilon_{\text{expt}}(\text{H}_2)$ in hydrogen-enriched C-H-Br compounds and solid carbon $\epsilon(C)$ in C-F-Br compounds will yield consistent results. This finding implies that $\epsilon(C)$ is different under certain circumstances, but that $\epsilon(\text{H}) = \frac{1}{2}\epsilon_{\text{expt}}(\text{H}_2)$ everywhere. (ii) The second alternative is that $\epsilon(C)$ is the same under all circumstances but that an $\bar{\epsilon}'(\text{H})$ must be used which differs by as much as 21% from $\frac{1}{2}\epsilon_{\text{expt}}(\text{H}_2)$. The second alternative gives consistent results in C-H-Br compounds if $\bar{\epsilon}'(\text{H})$ is used. Placing the entire blame on hydrogen, however, does not elucidate the very evident departures from Bragg's rule found by Bourland and Powers⁸ for C_2H_2 (which contains hydrogen) and CO (which does not contain hydrogen).

E. Iodine

To obtain $\epsilon(\text{I})$ from $\epsilon(\text{C}_2\text{H}_5\text{I})$ we used the same method described in Sec. IIID for the compound $\epsilon(\text{C}_2\text{H}_5\text{Br})$. There are seven combinations to obtain $\epsilon(\text{I})$ by subtracting the stopping cross sections of hydrocarbons from $\epsilon(\text{C}_2\text{H}_5\text{I})$. The probable errors of these seven values of $\epsilon(\text{I})$ range from $\pm(2.3-4.8\%)$:

$$(a) \quad \epsilon_1(\text{I}) = \epsilon(\text{C}_2\text{H}_5\text{I}) + \epsilon(\text{CH}_4) - \frac{3}{2}\epsilon(\text{C}_2\text{H}_6) \\ [\pm(2.8-4.8\%)],$$

$$(b) \quad \epsilon_2(\text{I}) = \epsilon(\text{C}_2\text{H}_5\text{I}) - \frac{1}{2}\epsilon(\text{C}_2\text{H}_4) - \frac{1}{2}\epsilon(\text{C}_2\text{H}_6) \\ [\pm(2.3-4.3\%)],$$

$$(c) \quad \epsilon_3(\text{I}) = \epsilon(\text{C}_2\text{H}_5\text{I}) - \frac{3}{4}\epsilon(\text{C}_2\text{H}_4) - \frac{1}{2}\epsilon(\text{CH}_4) \\ [\pm(2.4-4.4\%)],$$

$$(d) \quad \epsilon_4(\text{I}) = \epsilon(\text{C}_2\text{H}_5\text{I}) - \frac{1}{2}\epsilon(\text{CH}_4) - \frac{1}{2}\epsilon(\text{C}_3\text{H}_8) \\ [\pm(2.3-4.4\%)],$$

$$(e) \quad \epsilon_5(\text{I}) = \epsilon(\text{C}_2\text{H}_5\text{I}) - \frac{1}{2}\epsilon(\text{C}_2\text{H}_6) - \frac{1}{3}\epsilon(\text{C}_3\text{H}_8) \\ [\pm(2.3-4.3\%)],$$

$$(f) \quad \epsilon_6(\text{I}) = \epsilon(\text{C}_2\text{H}_5\text{I}) - \epsilon(\text{C}_2\text{H}_4) - \frac{1}{2}\epsilon(\text{H}_2) \\ [\pm(2.4-4.4\%)],$$

and

$$(g) \quad \epsilon_7(\text{I}) = \epsilon(\text{C}_2\text{H}_5\text{I}) - \epsilon(\text{C}_2\text{H}_6) + \frac{1}{2}\epsilon(\text{H}_2) \\ [\pm(2.4-4.4\%)].$$

All the $\epsilon_i(\text{I})$'s are consistent with each other within the quoted accuracies over the entire energy region 0.3-2.0 MeV.

$\epsilon(\text{I})$ can also be obtained by

$$\epsilon_8(\text{I}) = \epsilon(\text{C}_2\text{H}_5\text{I}) - 2\epsilon(\text{C}) - \frac{5}{2}\epsilon(\text{H}_2).$$

When solid $\epsilon(C)$ and $\epsilon(\text{H}_2)$ are used, $\epsilon_8(\text{I})$ is higher by as much as 9.8% than the above seven $\epsilon(\text{I})$ values. When hydrocarbon-gas $\epsilon(C)$ and $\epsilon(\text{H}_2)$ are used, $\epsilon_8(\text{I})$ has an accuracy of $\pm(2.6-4.4\%)$ and agrees with all $\epsilon_i(\text{I})$ ($i=1-7$). It essentially represents the weighted average of $\epsilon_i(\text{I})$ ($i=1-7$). We can also obtain

$$\epsilon_9(\text{I}) = \epsilon(\text{C}_2\text{H}_5\text{I}) - 2\epsilon_{\text{solid}}(\text{C}) - 5\bar{\epsilon}'(\text{H}),$$

where $\bar{\epsilon}'(\text{H})$ is given in Fig. 3. $\epsilon_9(\text{I})$ agrees to $\epsilon_8(\text{I})$ better than 0.3% everywhere except at 0.4 MeV where the agreement is 0.6%. We have taken $\epsilon_8(\text{I})$ to be the atomic stopping cross section of α particles in iodine and list it along with its probable error in Table IV.

IV. DISCUSSION

A. Bragg-Rule Applicability

The experiment of Bourland, Chu, and Powers showed that $\epsilon(C)$ measured in vapor-deposited solid C was different from $\epsilon(C)$ calculated by Bragg's rule from hydrocarbon gases. A possible physical-state effect would account for the observed discrepancy.

In the present experiment all stopping compounds are in the gaseous (or vapor) state, and contrary to our expectations, $\epsilon(C)$ obtained from fluoro-

carbon gases did not agree with hydrocarbon gas $\epsilon(C)$. This observation greatly weakens the assumption that a physical-state effect is possibly the cause of deviation from Bragg's rule, and may even imply that the problem is not due to a difference in $\epsilon(C)$ under certain circumstances but rather that the atomic stopping cross section $\epsilon(H)$ may be considerably different than one-half the molecular stopping cross section $\epsilon(H_2)$, as has usually been assumed in the past. If it is indeed true that $\epsilon(H)$ is not $\frac{1}{2}\epsilon(H_2)$, it is still puzzling why Bourland and Powers were able to apply Bragg's rule to $\epsilon(CH_4)$, $\epsilon(C_2H_4)$, $\epsilon(C_2H_6)$, $\epsilon(C_3H_8)$, and $\epsilon((CH_2)_3)$, solve pairs of Bragg-type equations for these compounds simultaneously, and obtain an $\epsilon(H)$ which agreed completely with the experimentally measured $\frac{1}{2}\epsilon_{\text{expt}}(H_2)$. The present experiment points out two alternatives: (i) Either solid $\epsilon(C)$ and an $\bar{\epsilon}'(H)$ which is not $\frac{1}{2}\epsilon_{\text{expt}}(H_2)$ can be used, or (ii) $\frac{1}{2}\epsilon_{\text{expt}}(H_2)$ can be used, but hydrocarbon-gas-carbon $\epsilon(C)$ must be used in hydrogen-enriched

C-H-Br or C-H-I compounds and solid-carbon $\epsilon(C)$ must be used in C-F, C-Cl, or C-F-Br compounds. It is clear that the *a priori* approach of measuring solid carbon $\epsilon(C)$ and gas $\epsilon_{\text{expt}}(H_2)$ and then using these results to predict molecular stopping cross sections is untenable under several circumstances.

Bragg-rule applicability can nevertheless be checked if a proper $\epsilon(C)$ or proper $\epsilon(H)$ is used. In our case we took the stopping cross section of the individual elements (Table IV), $\epsilon(H)$ [either $\frac{1}{2}\epsilon_{\text{expt}}(H_2)$ or $\bar{\epsilon}'(H)$], and $\epsilon(C)$ [solid $\epsilon(C)$ or hydrocarbon-gas $\epsilon(C)$ depending on whether the compound is hydrogen enriched or not], to compute the $\epsilon(\text{compound})$ according to the additivity rule. In making these calculations it is essential to follow either of the two alternatives outlined in the previous paragraph. This checking of the additivity rule, while appearing to be a rehashing of what has already been presented, is desirable since $\bar{\epsilon}(F)$, $\bar{\epsilon}(Cl)$, and $\bar{\epsilon}(Br)$ as given in Table IV

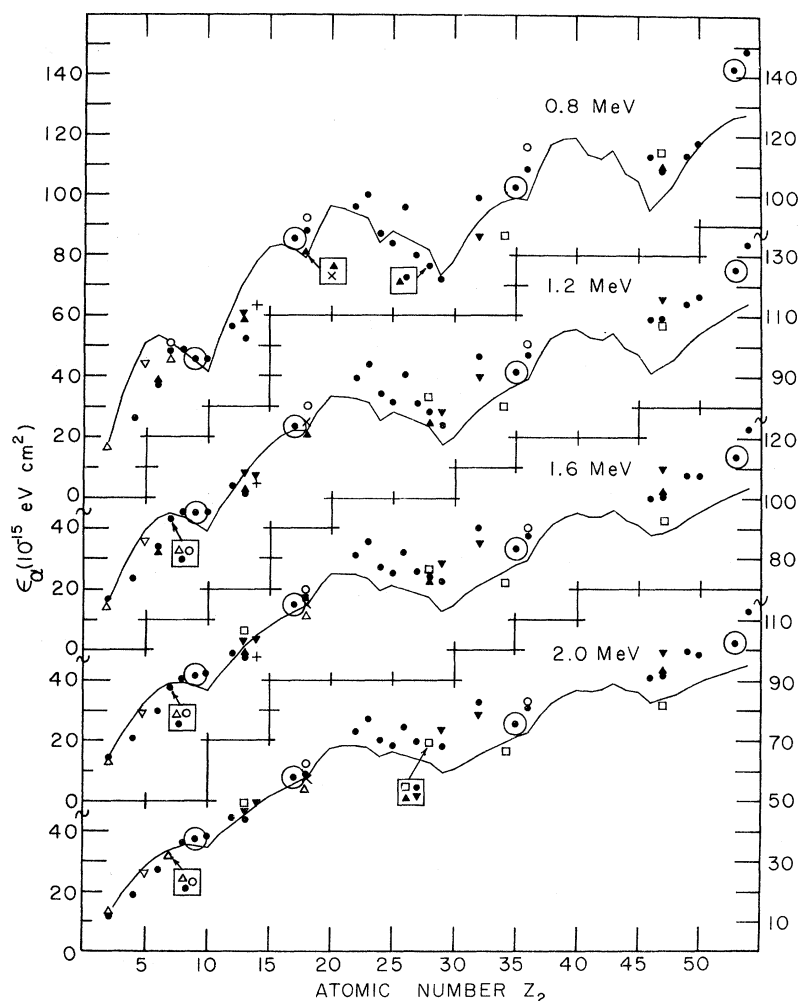


FIG. 5. Atomic stopping cross sections ϵ_α as a function of atomic number Z_2 of the stopping medium for α particles at energies 0.8, 1.2, 1.6, and 2.0 MeV. The solid curves are due to the theory of Lindhard and Winther (Ref. 14) as modified by Rousseau *et al.* (Ref. 7). Measurements at Baylor University (Refs. 5, 8, 9, and present experiment) are given by closed circles. The halogen measurements at $Z_2 = 9, 17, 35,$ and 53 are emphasized by enclosing them with large open circles. Other measurements are as follows: +, Thompson and Mackintosh (Ref. 15); \times , Weyl and Burgy as quoted by Porat and Ramavataram (Ref. 13); \blacktriangle , Porat and Ramavataram (Ref. 13); \blacktriangledown , Gobeli (Ref. 16); \triangle , Hoyer and Waeffler (Ref. 17); \circ , Kerr *et al.* (Ref. 18); \square , Nakata (Ref. 19); \blacksquare , Hanke and Bichsel (Ref. 20); ∇ , Kamke and Kramer (Ref. 21).

are weighted averages. It is possible that a molecular ϵ calculated from these weighted averages may deviate from a particular molecular ϵ . All molecular stopping cross sections calculated from atomic stopping cross sections should agree with the molecular stopping cross sections obtained experimentally. The calculated molecular stopping cross sections have probable errors ranging ± 1.4 – 3.3% , and are in excellent agreement with the experimental measurements. The agreement is better than 3% in all 13 compounds at all energies 0.3 – 2.0 MeV. Typically, the agreement is better than 1% . The average deviation between the experimental stopping cross section and that calculated from constituent atomic stopping cross sections is 0.8% . Thus, one can still use Bragg's rule in a meaningful way to calculate molecular stopping cross sections from atomic stopping cross sections, but judicious caution should be used in deciding *which* atomic stopping cross section to use for $\epsilon(C)$.

B. Z_2 Dependence

One of the reasons for conducting the present experiment was to obtain atomic stopping cross

sections of the halogens to determine if the Z_2 dependence of ϵ varied according to the theory and was consistent with the atomic species contiguous in Z_2 to the halogens.

We present in Fig. 5 a plot of ϵ_α vs Z_2 at the α -particle energies 0.8 , 1.2 , 1.6 , and 2.0 MeV. All Baylor measurements, whether solid or gas, are given by closed circles. The α -particle measurements by other groups are given by the symbols listed in the figure caption. We have not included proton stopping cross sections in order not to clutter the figure. Proton measurements, however, are quite consistent with α -particle measurements as is pointed out in Refs. 5 and 8. The solid curves are due to the theory of Lindhard and Winther¹⁵ as modified by Rousseau *et al.*⁷ We have drawn large open circles about the halogen measurements at $Z_2=9$, 17 , 35 , and 53 . The agreement of the present measurements with the general trend of ϵ_α vs Z_2 is most encouraging. Figure 5 also indicates very clearly that the trends predicted by the theory are substantiated by the experimental evidence. Preliminary measurements at Baylor on Y ($Z_2=39$) and Zr ($Z_2=40$) confirm the existence of a peak at $Z_2 \approx 40$; these findings will be presented in a forthcoming publication.

*Research supported by the Robert Welch Foundation, Houston, Texas 77002.

¹D. W. Green, J. N. Cooper, and J. Harris, *Phys. Rev.* **98**, 466 (1955).

²M. Bader, R. E. Pixley, F. S. Mozer, and W. Whaling, *Phys. Rev.* **103**, 32 (1956).

³K. R. MacKenzie, *Natl. Acad. Sci.—Natl. Res. Council Publ. No. 752* (1960).

⁴H. H. Andersen, C. C. Hanke, H. Simonsen, H. Sørensen, and P. Vajda, *Phys. Rev.* **175**, 389 (1968); H. H. Andersen, H. Sørensen, and P. Vajda, *ibid.* **180**, 373 (1969).

⁵W. K. Chu and D. Powers, *Phys. Rev.* **187**, 478 (1969).

⁶W. White and R. M. Mueller, *Phys. Rev.* **187**, 499 (1969).

⁷C. C. Rousseau, W. K. Chu, and D. Powers, *Phys. Rev. A* **4**, 1066 (1971); W. K. Chu and D. Powers, *Phys. Letters* **38A**, 267 (1972).

⁸P. D. Bourland, W. K. Chu, and D. Powers, *Phys. Rev. B* **3**, 3625 (1971); P. D. Bourland and D. Powers, *ibid.* **3**, 3635 (1971).

⁹W. K. Chu and D. Powers, *Phys. Rev. B* **4**, 10

(1971).

¹⁰R. B. J. Palmer, *Proc. Phys. Soc. (London)* **78**, 766 (1961).

¹¹James A. Phillips, *Phys. Rev.* **90**, 532 (1953).

¹²W. Whaling, in *Handbuch der Physik*, edited by S. Flügge (Springer-Verlag, Berlin, 1958), Vol. 34, p. 193.

¹³D. I. Porat and K. Ramavataram, *Proc. Phys. Soc. (London)* **78**, 1135 (1961).

¹⁴Jens Lindhard and Aage Winther, *Kgl. Danske Videnskab. Selskab, Mat.-Fys. Medd.* **34**, No. 4 (1964).

¹⁵D. A. Thompson and W. D. Mackintosh, *J. Appl. Phys.* **42**, 396 (1971).

¹⁶G. W. Gobeli, *Phys. Rev.* **103**, 275 (1956).

¹⁷U. Hoyer and H. Waeffler, *Z. Naturforsch.* **A26**, 592 (1971).

¹⁸G. D. Kerr, L. M. Hairr, N. Underwood, and A. W. Waltner, *Health Phys.* **12**, 1475 (1966).

¹⁹H. Nakata, *Phys. Rev. B* **3**, 2847 (1971).

²⁰C. C. Hanke and H. Bichsel, *Kgl. Danske Videnskab. Selskab, Mat.-Fys. Medd.* **38**, No. 3 (1970).

²¹D. Kamke and P. Kramer, *Z. Physik* **168**, 465 (1962).